

# A Histologic Study of the Extracellular Matrix During the Development of Glomerulosclerosis in Murine Chronic Graft-versus-Host Disease

E. C. Bergijk, C. Munaut, J. J. Baelde, F. Prins,  
J. M. Foidart, P. J. Hoedemaeker,  
and J. A. Bruijn

From the Department of Pathology, University of Leiden,  
Leiden, The Netherlands, and the Department of Biology,  
University of Liège, Liège, Belgium

*The development of glomerulosclerosis was studied in murine chronic graft-versus-host disease (GvHD), which is a model for human systemic lupus erythematosus. The authors investigated the distribution patterns of six components of the extracellular matrix (ECM), i.e., laminin, fibronectin, collagen types I, III, IV, and VI during the course of the disease. All of these ECM components except collagen type I were found in the glomeruli of normal mice, where all of them were intrinsic constituents of the mesangium. Laminin, fibronectin, and collagen type IV were also found in the glomerular capillary walls. Starting 6 weeks after the induction of GvHD and continuing at week 8, the onset of an expansion of the mesangial matrix was observed. At the same time, the amounts of laminin, fibronectin, and collagen types IV and VI increased. Ten weeks after the onset of the disease, glomerulosclerosis developed. Traces of the interstitial collagen type I were found in sclerotic glomeruli. The levels of four ECM components, i.e., collagens III, IV, VI, and laminin were markedly decreased in the sclerotic glomeruli as compared with week 8. In contrast, the amount of fibronectin in the sclerotic glomeruli increased dramatically. Immunoelectron microscopic examination showed fibronectin in the sclerotic lesions, in contrast to laminin, collagen type I, and collagen type IV. It is concluded that the sclerotic lesions in murine chronic GvHD contain fibronectin. The small amounts of the ECM components laminin, as well as collagens III, IV, and VI in the sclerotic glomeruli in GvHD, might represent remnants of mesangial material and collapsed capillary walls. These components are probably replaced by increased production and/or accumulation of col-*

*lagen type I and fibronectin. (Am J Pathol 1992, 140:1147-1156)*

Progressive glomerular sclerosis is a severe complication of many forms of renal disease. In the course of this process, structures in the glomerulus are replaced by fibroblasts and matrix.<sup>1</sup> This in turn leads to impairment of the filtration function of the kidney. Not much is known about the underlying mechanisms. Hemodynamic and genetic factors may play a role.<sup>2,3</sup> Interleukin 1 and transforming growth factor- $\beta$  are known to stimulate extracellular matrix (ECM) production by glomerular cells and have been postulated to play a central role in the pathogenesis of glomerulosclerosis.<sup>4-6</sup> A better understanding of the development of glomerulosclerosis will improve diagnosis and treatment in patients. Research in this field has focused on experimental models.

Murine graft-versus-host disease (GvHD) can be used as a model for systemic lupus erythematosus in humans.<sup>7</sup> GvHD is induced by transfer of DBA/2 lymphocytes into (C57BL/10 $\times$ DBA/2)F1 hybrids. This leads to an alloimmune reaction of parental T lymphocytes activated by H-2-incompatible structures of the recipient mice.<sup>8,9</sup> According to Via and Shearer,<sup>10</sup> the disease is the result of a deficient cytotoxic T-cell response in the DBA/2-derived inoculate. This leads to uncontrolled proliferation of autoantibody-producing B cells in the host.<sup>11</sup> The result is an SLE-like syndrome in which severe immune-complex glomerulonephritis (ICGN) is one of the major symptoms. In this model, ICGN is characterized by deposition of autoantibodies in the mesangium and along the GBM, resulting in thickening of the GBM, the formation of spikes and expansion of the mesangial matrix. From week 10 on, the development of glomerulosclerosis can be observed by light microscopic examination and

---

Supported by a grant from the Dutch Kidney Foundation (C89-847).

Accepted for publication December 26, 1991.

Address reprint requests to Dr. E. C. Bergijk, Department of Pathology, University of Leiden, P.O. Box 9603, 2300 RC Leiden, The Netherlands.

leads to severe renal failure and finally to the death of the animal.

Molecular dissection of the ECM in humans and laboratory animals, suggested that the sclerotic process is characterized by an abnormal production of ECM components.<sup>12-14</sup> To obtain more insight into the pathogenesis of glomerulosclerosis in our model of experimental lupus nephritis, we successively investigated the deposition patterns of the ECM components laminin, fibronectin, and collagen types I, III, IV, and VI. For this purpose, we used the techniques of immunofluorescence, immunoelectron microscopic examination, and the recently developed technique of reflection-contrast microscopy with peroxidase staining. This new technique provides enhanced detection sensitivity in immunostaining<sup>15</sup> and has not been previously applied for the study of glomerulosclerosis.

## Methods

### Animals

C57BL/10 (H-2b/b) and DBA/2 (H-2d/d) mice were purchased from Olac 1976 Ltd. (Bicester, Oxfordshire OX6 OTP, UK). (C57BL/10\*DBA/2)F1 hybrid mice were bred in our animal facilities. Female DBA/2 mice aged 7 to 8 weeks served as donors. Female F1 hybrids aged 8 to 10 weeks served as recipients. For the present study, we used 25 experimental F1 mice and 5 age- and sex-matched control mice.

### Induction of GvHD

Spleens, lymph-nodes (mesenteric, cervical, and inguinal), and thymi from DBA/2 donors were removed under aseptic conditions. Single-cell suspensions were prepared by mincing the tissue in sterile RPMI 1640 and gently pressing the fragments through a steel sieve (150  $\mu\text{m}$  pore diameter). The suspensions were filtered through a nylon sieve (71  $\mu\text{m}$  pore diameter), after which the cells were passed through a sterile Pasteur pipette loosely packed with cotton wool. The suspensions were washed twice in RPMI 1640 medium and centrifuged for 10 minutes at 250g. The pellets were resuspended in RPMI 1640. The total number of cells and the proportion of vital cells were determined by Trypan blue exclusion and phase-contrast microscopic examination. The suspensions were washed again, and the pellets were resuspended in Hanks' balanced salt solution (HBSS). The suspensions were mixed. On days 0, 3, 7, and 10, the F1 recipients were injected intravenously with  $50 \times 10^6$  viable DBA/2 cells in 0.25 ml HBSS. The dose was composed of

approximately 60% spleen cells, 30% thymocytes, and 10% lymph-node cells. Control mice were injected simultaneously with 0.25 ml phosphate-buffered saline (PBS).

### Follow-up of F1 Mice

The albumin content of the urine of the GvHD F1 and control mice was determined 1 week before and 2 weeks after the first injection of parental cells and then at two-weekly intervals. The animals had been kept in urine-collection cages for 18 hours with free access to water and food. The albumin level was assessed by rocket electrophoresis against rabbit anti-mouse albumin, which had been produced by immunization of a rabbit with purified mouse serum albumin (Sigma Chemical Corporation, St. Louis, MO). This mouse albumin was also used as standard.<sup>16</sup> After urine collection, the mice were anesthetized with diethylether and blood was collected from the orbital plexus. Serum samples were prepared and tested to detect the presence of autoantibodies.<sup>9</sup> The direct Coomb's test was used to assess the *in vivo* fixation of immunoglobulins by erythrocytes.<sup>9</sup> Groups of five mice each were killed every other week starting at week 4 and ending at week 12. After perfusion with Dulbecco's phosphate-buffered saline (PBS), the kidneys were removed. Small pieces of kidney tissue were embedded in Lowicryl for electron and reflection microscopic examination. Some of the tissue was fixed in 10% buffered formalin, dehydrated, and then embedded in Paraplast<sup>®</sup> (Amstelstad, Amsterdam, The Netherlands) for light microscopic examination. The remaining kidney tissue was frozen in CO<sub>2</sub> ice-cooled isopentane and stored at  $-70^\circ\text{C}$  until use for the immunofluorescence studies. For electron and reflection microscopic examination, the kidneys were perfusion-fixed with paraformaldehyde and 0.25% glutaraldehyde in 0.1 mol/l PBS, and embedded in Lowicryl.

### Antibodies

We used rabbit-anti-mouse IgG obtained from Janssen (Olen, Belgium), affinity-purified goat-anti-type I, anti-type III, and anti-type IV collagen antisera from Sera-lab (Sussex, England), rabbit-anti-EHS laminin from E-Y laboratories (San Mateo, CA), polyvalent rabbit serum against type VI collagen from Heyl (Berlin, Germany), and polyclonal antiserum to human fibronectin from Sigma (St Louis, MO). As second antibodies in the immunofluorescence studies, we used FITC-labeled goat-anti-rabbit IgG and rabbit-anti-goat IgG from Nordic (Tilburg, The Netherlands). For reflection contrast microscopic examination, we used peroxidase-labeled swine anti-rabbit

and peroxidase-labeled swine anti-goat antibodies (DAKO, Denmark) and gold-labeled goat-anti-rabbit-G15 as second-step antibodies (Amersham). In the immunoelectron microscopic studies, rabbit-anti-goat IgG was used as second antibody. Gold-labeled goat-anti-rabbit-G15 was used as third antibody, and as second antibody in laminin staining. Specificities were determined using indirect and direct ELISA, indirect immunofluorescent staining, indirect immunocytochemical analysis, and dot blotting techniques.

### *Histologic Techniques*

The kidney tissue was processed for light microscopic and immunofluorescence studies as described elsewhere.<sup>17</sup> The light-microscopic slides were stained with periodic acid-Schiff (PAS) or hematoxylin-eosin (H&E). The immunofluorescence slides were scored double-blind by two observers independently of each other. Immunoelectron microscopic examination was completed according to Abrahamson et al.<sup>18</sup> On the grids the sections were poststained with uranyl acetate and Reynold's lead citrate, and examined in a Philips CM10 electron microscope, operating at 60 kV. Reflection-contrast microscopic examination and postembedding histochemical analysis were done according to Cornelese-ten Velde et al.<sup>15</sup> with a few modifications. Briefly, the kidneys were perfusion-fixed with 1% paraformaldehyde and 0.25% glutaraldehyde in 0.1 mol/l PBS (pH 7.4). Dehydration and embedding were performed according to Altman et al.<sup>19</sup> Ultrathin sections ( $\pm 80$  nm) were caught on aminocyclane-coated slides. The slides were then preincubated in 1% bovine serum albumin (BSA) in PBS, and reincubated overnight at 4°C with the first antibody. The second antibody was incubated for 2 hours. When a peroxidase-labeled second antibody had been used, the sections were incubated 10 minutes in a solution of 50 mg/100 ml diaminobenzidine and 0.01% hydrogen peroxide in 0.05 mol/l TRIS-HCl (pH 7.6). The slides were washed in PBS and in double-distilled water, before being examined. The slides were not counterstained or covered with a coverslip.

## **Results**

### *Development of GvHD*

The albumin excretion of the diseased animals rose sharply and reached the highest levels in week 12 ( $30,000 \pm 2,140 \mu\text{g}/18 \text{ hr}$  vs  $40 \pm 2 \mu\text{g}/18 \text{ hr}$  for the control mice). Ascites and edema developed in the majority of the treated animals. Antinuclear antibodies devel-

oped in all treated animals. In the course of the disease, 92% of the animal sera became positive in the direct Coomb's test, indicating the development of autoimmunity. Light and electron microscopic examinations showed a lupus type of nephritis with glomerular proliferation as well as membranous nephritis, complicated by glomerular sclerosis starting 10 weeks after the induction of GvHD. At this stage, Bowman's capsule was markedly thickened, especially at the hilus. Furthermore adhesions were seen between the visceral and parietal glomerular epithelia.

The glomerular deposition patterns of the ECM molecules were determined semiquantitatively by immunofluorescence techniques. The results are summarized in Table 1. We also studied the localization patterns of laminin, fibronectin, collagen type I, and type IV, and the IgG deposits at the ultrastructural level, using reflection-contrast and immunoelectron microscopic examinations. Four sequential ultrathin sections of material representing GvHD week 10 material were cut, immediately followed by a section with a thickness of 0.5  $\mu\text{m}$ . The ultrathin slides were stained with antibodies against IgG, laminin, collagen IV, and fibronectin. The thicker section was given a PAS-staining. The results are shown in Figure 2. On this basis conclusions could be drawn concerning the distribution of these ECM components in relation to the IgG-containing deposits and the sclerotic lesions. The signals of the other ECM components studied were too weak for detection by these methods.

### *IgG Deposits*

The immunofluorescence and reflection-contrast microscopic studies showed IgG in a mainly linear pattern along the glomerular capillary wall, starting 2 weeks after the induction of GvHD. The distribution of IgG changed to a more granular pattern after 6 to 8 weeks. At this stage, the kidneys of diseased animals showed electron-dense deposits in the mesangium and subepithelially along the glomerular capillary wall at the ultrastructural level. Incubation with anti-IgG antibodies led to staining of the electron-dense deposits (Figure 1). The GBM showed irregular thickening with formation of spikes. With the development of glomerular sclerosis, the presence of IgG at the sites of the sclerotic lesions decreased (Figure 2b). Immunoelectron microscopic examination showed few deposits of IgG in the sclerotic lesions as compared with the presence of IgG in the electron-dense deposits in the remnants of the mesangial matrix and GBM (Figure 3a).

Laminin was localized in the mesangium and the glomerular capillary wall in normal mice (Figure 2e). Six weeks after the induction of GvHD, the amount of laminin in the mesangium as well as that in the glomerular cap-

**Table 1. Deposition of Extracellular Matrix Molecules in Kidneys of Mice Suffering from GuHD, as Determined Semiquantitatively by Immunofluorescence Studies**

		lam	col I	col III	col IV	col VI	fn
nF1	mes	++	-	+	++	+	++
	GCW	+	-	-	±	-	+
	BC	+	±	+	++	+	+
	TBM	++	±	±	++	+	++
	int	+	+	++	-	-	+
wk 4	mes	++	-	+	++	+	++
	GCW	+	-	-	±	-	+
	BC	+	±	+	++	+	+
	TBM	++	±	±	++	+	++
	int	+	+	++	-	-	+
wk 6	mes	+++	-	+	+++	+/++	+++
	GCW	+/++	-	-	±	-	++
	BC	++	±	+	++	+	+
	TBM	++	±	±	++	+	+
	int	+	+/++	++	±	-	+
wk 8	mes	+++	-	+	+++	+/++	+++
	GCW	+/++	-	-	+	-	++
	BC	++	±	+	++	+	+
	TBM	++	±	±	++	+	+
	int	+	+/++	++	±	-	+
wk 10/12	gsl	-	-	-	-	-	++++
	mes	+++	+	+	+++	+/++	+++
	GCW	+/++	-	-	+	-	++
	BC	+++	+	+	++	+	++
	TBM	++	+	±	+++	+	+
	int	++	+++	+++	+	++	+

mes = mesangium, GCW = glomerular capillary wall, BC = Bowman's capsule, TBM = tubular basement membrane, int = interstitium, gsl = glomerular sclerotic lesion, lam = laminin, col I = collagen type I, fn = fibronectin.

illary wall increased (Figure 2f). Two weeks later, the localization of laminin had not changed. At week 10, however, the distribution of laminin changed radically at the sites where glomerulosclerosis developed. In the mesangial areas that were not yet sclerotic, the laminin distribution was the same as at week 8. However, in the sclerotic regions the presence of laminin was dramatically decreased relative to the occurrence at week 8 (Figure 2g).

Immunoelectron microscopic examination at weeks 6 and 8 showed laminin around the deposits, and concentrated mainly at the top of the spikes (Figure 3b). In sclerotic glomeruli at week 10, laminin was found in mesangial and capillary material around the sclerotic lesions (Figure 3c).

Collagen I was found in small amounts in the interstitium, the tubular basement membrane (TBM), Bowman's

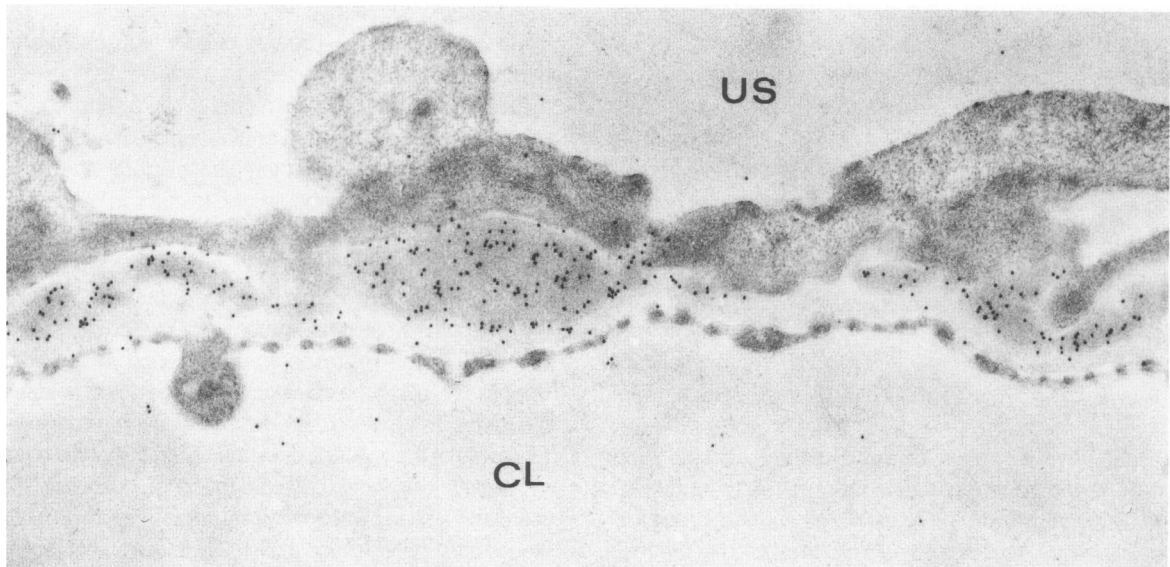


**Figure 1. Electronmicrograph of the glomerular basement membrane of a mouse 8 weeks after induction of GuHD. The electron-dense deposits react with anti-IgG antibodies (×23000). US = urinary space; CL = capillary lumen.**

capsule, and more abundantly in vessel walls, but not in the glomerular capillary network of normal F1 mice. Up to 8 weeks after the onset of the disease, a slight increase in the interstitium, the TBM, and Bowman's capsule occurred. Starting at week 10, traces of collagen I were seen in the glomeruli. At that time there was a dramatic increase of this type of collagen in the interstitium, the TBM, and Bowman's capsule (Figure 4). Immunoelectron microscopic examination at week 10 showed small amounts of collagen type I in the mesangial matrix, but not in the glomerular sclerotic lesions (Figure 3d).

Collagen III was found in the mesangium of glomeruli of normal mice. There was no staining of the glomerular capillary wall. In the course of the disease, staining of the mesangium showed no to a slight increase. Sclerotic glomeruli at week 10 showed a decrease of collagen III (Figure 5). The sclerotic regions did not stain for collagen type III. Compared with normal glomeruli, the amount of collagen III increased, especially interstitially, after GvHD induction.

Collagen IV was present in the mesangium and the glomerular capillary wall of normal mice. Bowman's capsule was also strongly positive for collagen type IV. Starting at week 6 the amount of collagen IV in the mesangium increased. At weeks 10 and 12, in the sclerotic lesions, the amount of collagen type IV was smaller than it had been in week 8. Parts of the glomeruli that had not yet become sclerotic, showed a distribution pattern similar to that seen in week 8 (Figure 2c).

Immunoelectron microscopic examination showed collagen type IV in the mesangial matrix and in the glomerular capillary wall around the electron-dense deposits at week 6 and 8. In sclerotic glomeruli, collagen type IV was present in the mesangial matrix and the remainders of the GBM, but not in the sclerotic lesions (Figure 3e).

Collagen VI was found in the mesangium, Bowman's capsule, the TBM, and around the vessel walls in normal mice. Six weeks after the induction of the disease, expansion of the mesangium began and an increase of collagen type VI occurred. At weeks 10 and 12, a marked increase had occurred in the interstitium, especially around the vessel walls. In the glomeruli, collagen VI had almost totally disappeared. Nonsclerotic parts of glomeruli showed mesangial staining resembling that seen at week 8 (Figure 6).

Fibronectin was found both in the mesangium and the glomerular capillary wall of control mice. Bowman's capsule and the TBM were positive. Six weeks after the onset of GvHD, fibronectin increased in the mesangium, but remained unchanged in the capillary wall. This picture persisted in week 8. The sclerotic glomeruli appearing at week 10 showed a large amount of fibronectin (Figure 2d).

Immunoelectron microscopic examination showed a diffuse distribution of fibronectin in the sclerotic lesions.

Within the lesions, differences in the degree of electron density occurred. The more electron-dense material in the sclerotic lesions stained more intensely for fibronectin than the less electron-dense parts did. Fibronectin was also present in the mesangial matrix and in the remnants of GBM around the sclerotic lesions (Figure 3f).

## Discussion

In the present study, we investigated glomerular sclerosis as a complication of immunologically mediated glomerulonephritis. Improvement of the diagnosis and treatment of patients requires a better understanding of the mechanisms underlying the development of glomerulosclerosis. To this end, we studied the distribution patterns of a number of extracellular matrix components, i.e., laminin, fibronectin, and collagen types I, III, IV, and VI in the experimental murine GvHD model, making use of immunofluorescence, immunoelectron microscopy, and the recently developed technique of reflection-contrast microscopy with peroxidase staining. The reflection-contrast microscopic technique offers a useful supplement to the well-known technique of immunofluorescence. The detection level of the former method is slightly lower, because less antigen is present in the ultrathin sections.<sup>15</sup> However, the staining is much more precise. The minimal thickness of these sections makes it possible to define a sequential range of serial sections through a single glomerulus. The morphology shown by these ultrathin sections is comparable, which means that the distribution patterns of the various ECM components can be compared in relation to each other and to immunoglobulins present.

In normal (C57BL/10\*DBA/2)F1 hybrid mice, we found the components laminin, fibronectin, collagen types III, IV, and VI, in the glomerular mesangium. Laminin, fibronectin, and in small amounts, collagen type IV, were also found in the glomerular capillary wall.

The finding of collagen type III in the glomeruli of normal mice is in itself remarkable. Most other authors did not find collagen type III in normal glomeruli of humans<sup>12,20,21</sup> or rats.<sup>13,22,23</sup> On the other hand, Downer et al<sup>24</sup> reported finding trace amounts of interstitial collagen in some glomeruli of control New Zealand White rabbits. Thus, differences in collagen III distribution might exist between species or even between strains.

The amounts of all the ECM components studied increased during the course of the disease. Changes began to occur 6 weeks after the induction of GvHD. At this stage, the mesangium started to expand. Irregular thickening of the GBM and the formation of spikes were also observed. IgG-containing electron-dense deposits were present both subendothelially and subepithelially along the GBM.



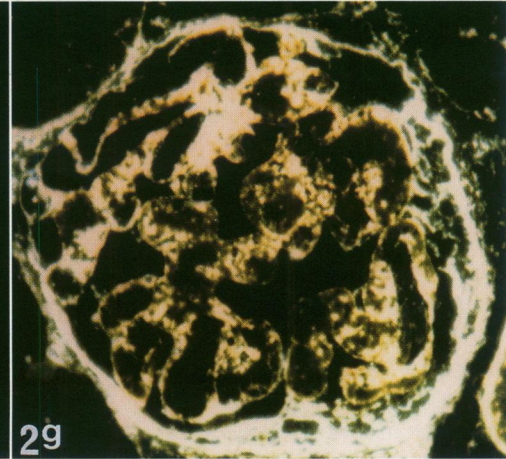
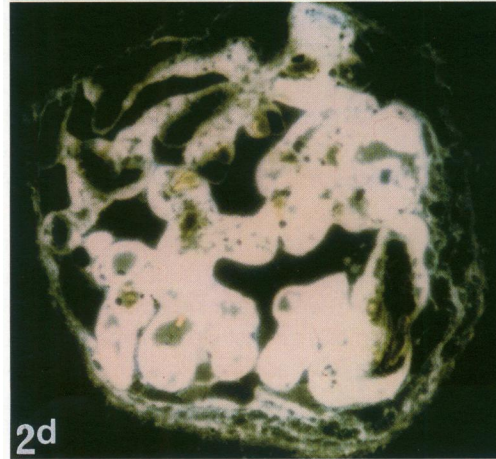
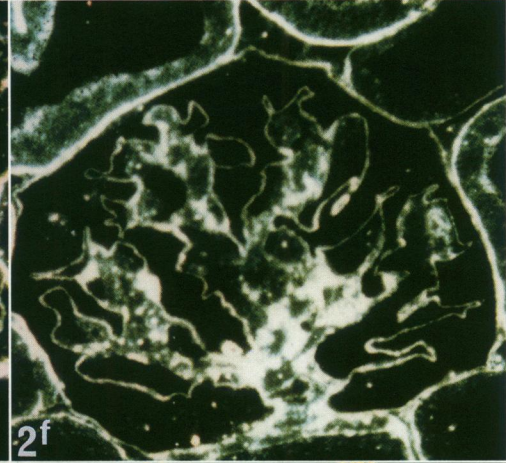
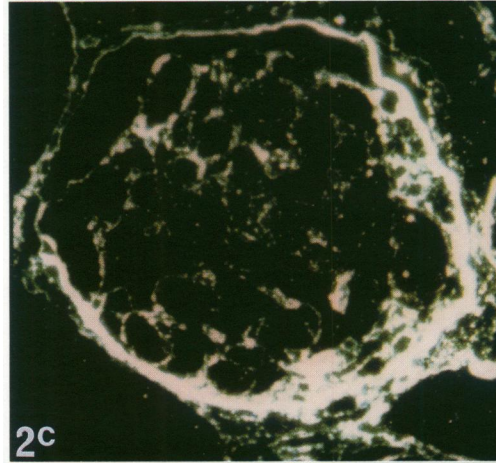
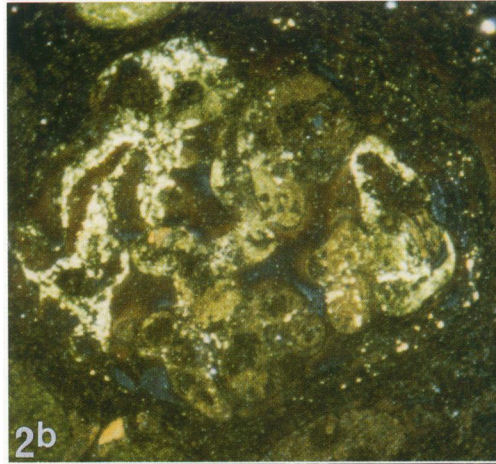
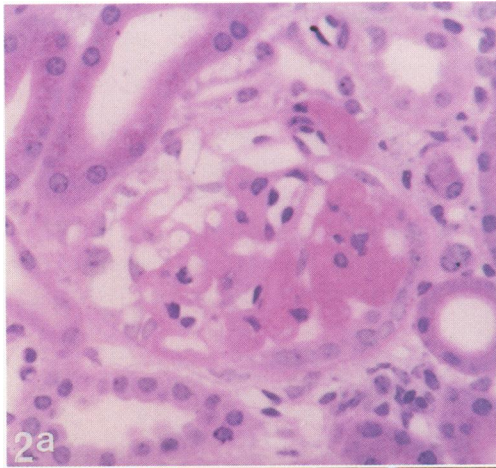


Figure 2. a: Glomerulus 10 weeks after the induction of GvHD, stained according to the PAS technique. b: IgG distribution in glomerulus at week 10. c: Collagen type IV at week 10. d: Fibronectin at week 10. e: Laminin distribution in a glomerulus of a normal F1 hybrid mouse. f: Laminin distribution 6 weeks after induction of GvHD. g: Laminin distribution at week 10; (a-d) and (g) show sequential sections of one glomerulus; (b-g) the peroxidase reflection contrast microscopical technique was used ( $\times 630$ ).

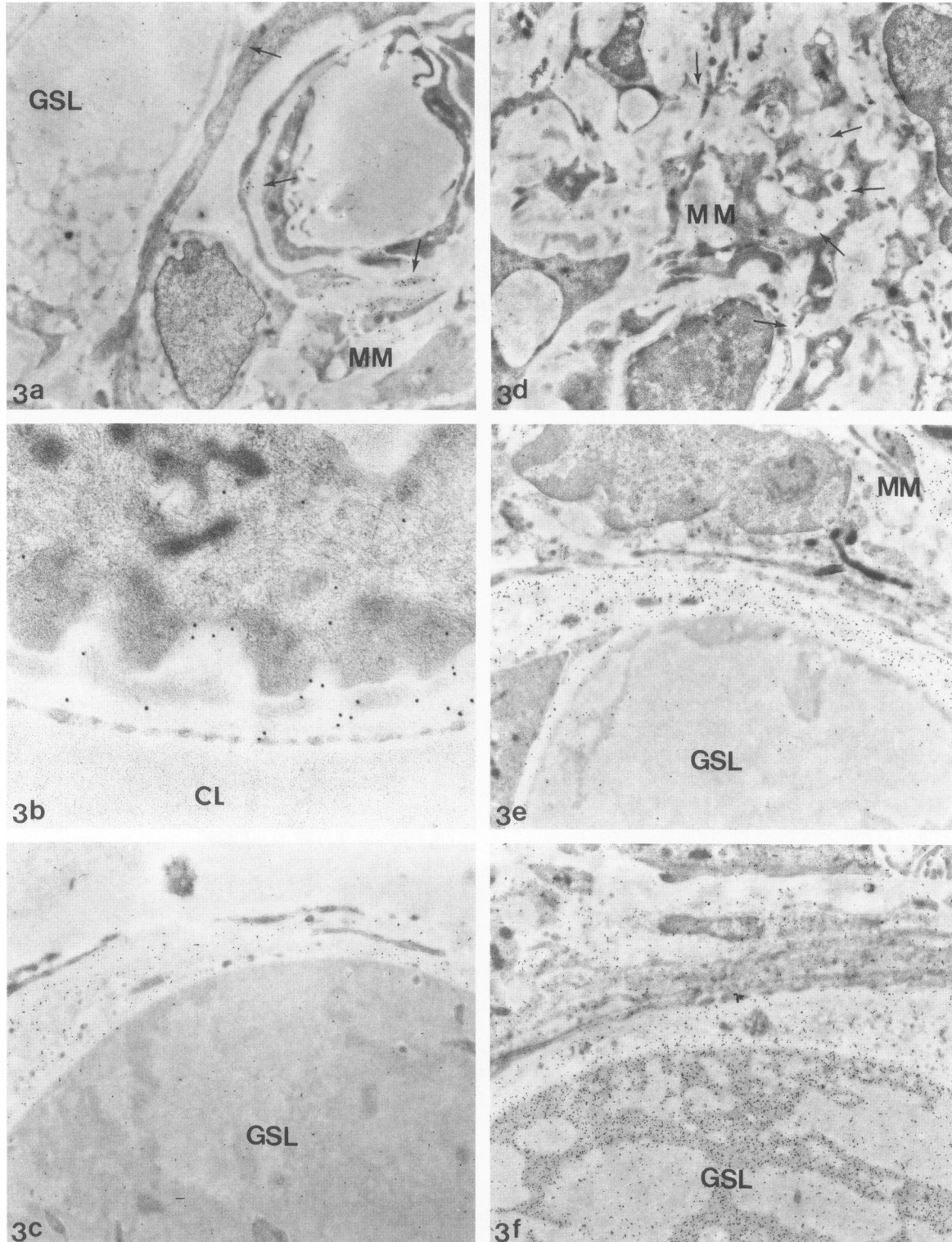
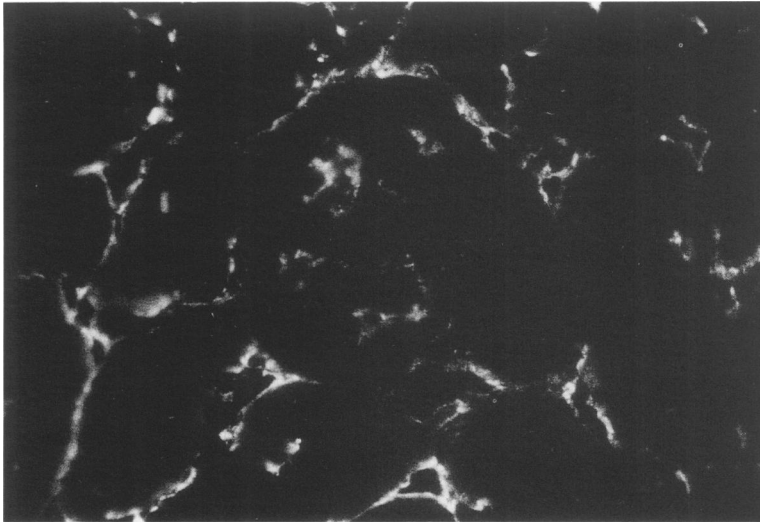


Figure 3. Immunoelectron micrographs of (a) IgG distribution in a glomerulus 10 weeks after the induction of GvHD, arrows indicate IgG containing electron-dense deposits; (b) glomerular basement membrane showing localization of laminin at week 8; (c) Laminin distribution at week 10; (d) collagen I (arrows) at week 10; (e) collagen IV at week 10; and (f) fibronectin at week 10. Magnification a, c-f,  $\times 7000$ ; b,  $\times 28000$ . GSL = glomerular sclerotic lesion, MM = mesangial matrix, CL = capillary lumen.





**Figure 4.** *Immunofluorescence micrograph showing the distribution pattern of collagen type I 10 weeks after GvHD induction ( $\times 630$ ).*

Starting 10 weeks after induction of the disease, glomerular sclerosis developed. This was associated with adhesion to and thickening of Bowman's capsule. The first striking finding was the appearance of traces of the interstitial collagen type I in the glomerulus at this timepoint. Our finding is in agreement with the observations made by Foellmer et al,<sup>16</sup> who suggested an association between the presence of collagen I and interruption of Bowman's capsule in rats with anti-GBM nephritis. A genotype switch of glomerular cells leading to local production of collagen type I has also been suggested as an explanation for the presence of interstitial collagens in a glomerulus.<sup>25</sup> Our finding of collagen type I in the mesangial matrix and not in the glomerular sclerotic lesions might be in agreement with this hypothesis. In addition, diminished collagenase I activity in sclerotic glomeruli cannot be ruled out as an explanation for the presence of collagen type I in sclerotic glomeruli. This could be due to damage of the cells producing this enzyme.

Second, we found striking differences between the distribution patterns of the ECM components in the sclerotic glomeruli. Fibronectin was present in the sclerotic lesions. The other components we investigated showed a sudden decrease relative to the level at week 8. We had the impression that these components were replaced by the sclerotic lesions. The traces of ECM components found around the lesions are believed to have been remnants of mesangial material and/or of collapsed capillary walls. The finding of differences in the occurrence of individual ECM molecules in sclerotic glomeruli is in itself interesting. Recently, Ikeda et al<sup>26</sup> found differences in the localization of various ECM components in diabetic glomerular lesions. They found that collagen IV occurred in the core portion of the nodular lesion, whereas collagen VI was seen in the surrounding laminated acellular area. These authors believed that the formation of the lesions in diabetic microaneurysms might be based on the increase of type VI collagen.

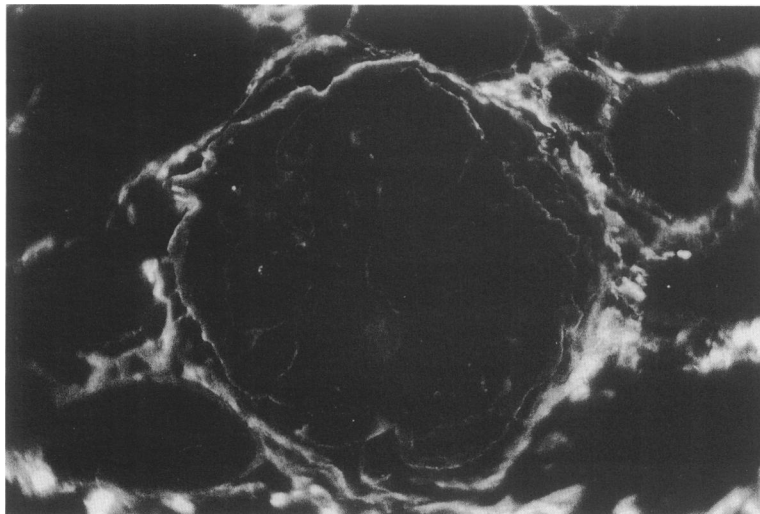


**Figure 5.** *Immunofluorescence micrograph showing the distribution pattern of collagen type III 10 weeks after GvHD induction ( $\times 630$ ).*



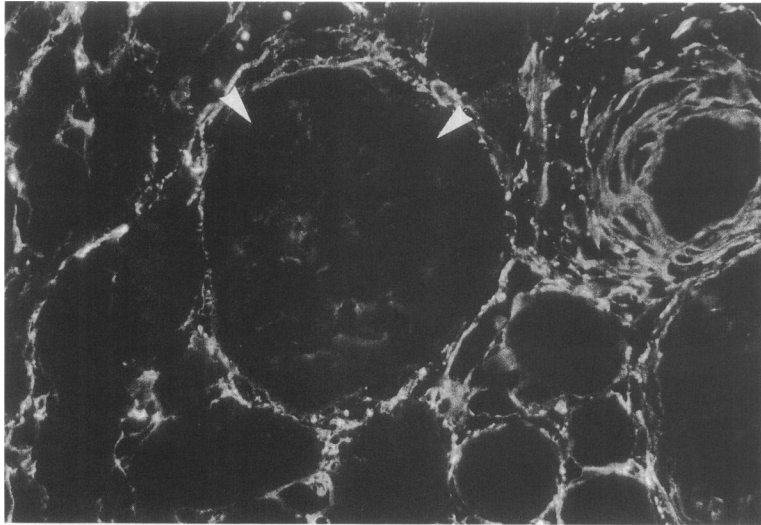


**Figure 6.** Distribution of type VI collagen in a sclerotic glomerulus 12 weeks after the induction of GvHD. Type VI collagen had almost disappeared in the sclerotic areas (arrowheads). Immunofluorescence micrograph ( $\times 630$ ).

Last year, Funabiki et al<sup>27</sup> reported fluorescence studies in patients with glomerulonephritis and diabetic nephropathy. In the advanced stages of glomerulonephritis, they found a marked increase of types IV and VI collagen, laminin, and fibronectin in the mesangium. The distribution extended along the glomerular capillary walls as well. During the progression of glomerulosclerosis, they found a significant decrease in the amount of type IV collagen, laminin, and fibronectin, whereas the occurrence of interstitial collagen types I and III was observed focally in the glomerular lesions.

The observed influx of collagen type I and the decreased amounts of laminin and collagen IV in our model in the sclerotic stage is comparable with Funabiki's findings in the aforementioned renal diseases. Markedly divergent, however, is our finding of fibronectin in the sclerotic lesions. Unfortunately, our model does not allow investigation of the composition of sclerotic lesions during the progression of glomerulosclerosis, because the mice do not live long enough.

The glomerular sclerotic lesions appeared to consist of material of variable electron density in immunoelectron microscopic examination as well as in routine electron microscopic examination. The more electron-dense parts of the lesions contained more fibronectin than the less electron-dense parts did. The sclerotic lesions in GvHD probably contain a variety of molecules. Albumin, transferrin, and fatty acids were not among them (unpublished results).

There are two possible explanations for the increased presence of fibronectin in the glomeruli of GvHD mice. First, there might be an accelerated increase of the synthesis and excretion of fibronectin or decreased breakdown during the development of glomerulosclerosis. The second hypothesis is that there is an accumulation of

exogenous fibronectin from the circulation. During the course of GvHD, a dramatic change in glomerular morphology was seen, including thickening of the glomerular capillary walls and narrowing of the capillary loops. This might lead to trapping of exogenous fibronectin and other components from the circulation into the glomerulus. The other ECM components might be pushed aside or covered by the accumulated material. The accumulation of fibronectin in the sclerotic lesions might be facilitated by fibronectin-binding receptors. Recently, a pilot study showed increased expression of adhesion molecules of the integrin family. Furthermore histologic staining for albumin, transferrin, and fatty acids showed that the development of glomerulosclerosis in murine chronic GvHD is not a process of nonspecific trapping of proteins from the circulation. However, it is accompanied by bloodclotting as shown by fibrin and fibrinogen staining (unpublished results).

Further investigations, including mRNA studies, are needed to establish which mechanisms underlie the development of glomerulosclerosis in murine chronic GvHD and the abnormal composition of the ECM in these lesions. We recently speculated about the nature of progression in experimental lupus nephritis.<sup>28</sup> Investigations in this field can contribute to a better understanding of the development of glomerulosclerosis, and thus to improvement of the diagnosis and treatment of patients with glomerulonephritis.

### Acknowledgments

The authors thank J. van der Ploeg for technical assistance and Dr. E. de Heer for stimulating discussions.

## References

1. Klahr S, Schreiner G, Ichikawa I: The progression of renal disease. *N Engl J Med* 1988, 318:1657–1666
2. El Nahas AM: Glomerulosclerosis: Insights into pathogenesis and treatment. *Nephrol Dial Transplant* 1989, 4:843–853
3. Weening JJ, Beukers JJB, Grond J, Elema JD: Genetic factors in focal segmental glomerulosclerosis. *Kidney Int* 1986, 29:789–798
4. Torbohm I, Berger B, Schönermark M, Von Kempis J, Rother K, Hänsch GM: Modulation of collagen synthesis in human glomerular epithelial cells by interleukin-1. *Clin Exp Immunol* 1989, 75:427–431
5. Border WA, Okuda S, Languino LR, Ruoslahti E: Transforming growth factor- $\beta$  regulates production of proteoglycans by mesangial cells. *Kidney Int* 1990, 37:689–695
6. Border WA, Okuda S, Languino LR, Sporn MB, Ruoslahti E: Suppression of experimental glomerulonephritis by antiserum against transforming growth factor beta-1. *Nature* 1990, 346:371–374
7. Bruijn JA, Van Elven EH, Hogendoorn PCW, Corver WE, Hoedemaeker PhJ, Fleuren GJ: Murine chronic graft-versus-host disease as a model for human lupus nephritis. *Am J Pathol* 1988, 130:639–641
8. Rolink AG, Gleichmann H, Gleichmann E: Diseases caused by reactions of T-lymphocytes to incompatible structures of the major histocompatibility complex. VII. Immune-complex glomerulonephritis. *J Immunol* 1983, 130:209–215
9. Van Elven EH: Reactions of T-cells cause SLE and related disorders. The Netherlands, University of Amsterdam, Krips Repro Meppel, 1981 (academic thesis)
10. Via CS, Shearer GM: T-cell interactions in autoimmunity: insights from a murine model of graft-versus-host disease. *Immunol Today* 1988, 9:207–213
11. Gleichmann E, Pals STP, Rolink AG, Radaszkiewicz T, Gleichmann H: Graft-versus-host reactions: clues to the etiopathology of a spectrum of immunological diseases. *Immunol Today* 1984, 5:324–332
12. Morel-Maroger Striker L, Killen PD, Chi E, Striker GE: The composition of glomerulosclerosis. Studies in focal sclerosis, crescentic glomerulonephritis, and membranoproliferative glomerulonephritis. *Lab invest* 1984, 51:181–192
13. Adler S, Striker LJ, Striker GE, Perkinson DT, Hibbert J, Couser WG: Studies of progressive glomerular sclerosis in the rat. *Am J Pathol* 1986, 123:553–562
14. Foellmer HG, Bernd-Sterzel R, Kashgarian M: Progressive glomerular sclerosis in experimental antiglomerular basement membrane glomerulonephritis. *Am J Kidney Diseases* 1986, VII:5–11
15. Comelese-ten Velde I, Prins FA: New sensitive light microscopical detection of colloidal gold on ultrathin sections by reflection contrast microscopy. *Histochemistry* 1990, 94:61–71
16. Axelsen NH: Quantitative immunoelectrophoresis, New developments and applications. *Scand J Immunol* 1975, Suppl 2
17. Bruijn JA, Hogendoorn PCW, Corver WE, Van den Broek LJC, Hoedemaeker PJ, Fleuren GJ: Pathogenesis of experimental lupus nephritis: a role for anti-basement membrane and anti-tubular brush border antibodies in murine chronic graft-versus-host disease. *Clin exp Immunol* 1990, 79:115–122
18. Abrahamson DR: Post-embedding colloidal gold immunolocalization of laminin to the lamina rara interna, lamina densa, and lamina rara externa of renal glomerular basement membranes. *J Histochem Cytochem* 1986, 34:847–853
19. Altman LG, Schneider BG, Papermaster DS: Rapid embedding of tissues in lowicryl k4m for immunoelectron microscopy. *J Histochem Cytochem* 1984, 32:1217–1223
20. Yoshika K, Takemura T, Tohda M, Akano N, Miyamoto H, Ooshima A, Maki S: Glomerular localization of type III collagen in human kidney disease. *Kidney Int* 1989, 35:1203–1211
21. Oomura A, Nakamura T, Arakawa M, Ooshima A, Isemura M: Alterations in the extracellular matrix components in human glomerular diseases. *Virchows Arch [A]* 1989, 415:151–159
22. Abrass CK, Peterson CV, Raugi GJ: Phenotypic expression of collagen types in mesangial matrix of diabetic and non-diabetic rats. *Diabetes* 1988, 37:1695–1702
23. Karkavelas G, Kefalides NA, Amenta PS, Martinez-Hernandez A: Comparative ultrastructural localization of collagen types III, IV, VI and laminin in rat uterus and kidney. *J Ultrastruc Mol Struc Res* 1988, 100:137–155
24. Downer G, Phan SH, Wiggins RC: Analysis of renal fibrosis in a rabbit model of crescentic nephritis. *J Clin Invest* 1988, 82:998–1006
25. Bruijn JA, Hogendoorn PWC, Hoedemaeker PJ, Fleuren GJ: The extracellular matrix in pathology. *J Lab Clin Med* 1988, 111:140–146
26. Ikeda K, Kida H, Oshima A, Takaeda M, Naito T, Yokoyama H, Tomosugi N: Participation of type III, IV and VI collagen fibers in formation of diabetic glomerular lesions. *Kidney Int* 1990, 37:440 (abstract)
27. Funabiki K, Horikoshi S, Tomino Y, Nagai Y, Koide H: Immunohistochemical analysis of extracellular components in the glomerular sclerosis of patients with glomerulonephritis. *Clin Nephrol* 1990, 34:239–246
28. Bruijn JA, Bergijk EC, De Heer E, Fleuren GJ, Hoedemaeker PJ: Induction and progression of experimental lupus nephritis: Exploration of a pathogenetic pathway. Editorial review. *Kidney Int* 1992, 41:5–13